J Electr Eng Technol.2018; 13(2): 761-768
http://doi.org/10.5370/JEET.2018.13.2.761

ISSN(Print) 1975-0102
ISSN(Online) 2093-7423

Direct Power Control of PMa-SynRG with Back-to-back PWM Voltage-fed Drive

Jeihoon Baek* and Sangshin Kwak†

Abstract – In this paper, the performance analysis of a control topology based on the direct output power control (DPC) for robust and inexpensive permanent magnet-assisted synchronous reluctance generator (PMa-SynRG) system is presented. The PMa-SynRG might be coupled to an internal combustion engine running at variable speed. A three-phase PWM rectifier rectifies the generator output and supplies the dc link. A single-phase PWM inverter supplies constant ac voltage at constant frequency to the grid. The overall control algorithm is implemented on a TMS320F2812 digital signal processor board. Simulations results and experimental results verify the operation of the proposed system.

Keywords: Back-to-back PWM voltage-fed drive, Direct power control (DPC), Permanent magnet-assisted synchronous reluctance generator (PMa-SynRG)

1. Introduction

A wide constant power-speed range (CPSR), high efficiency and high reliability are required from auxiliary generator systems for commercial and military applications [1]. Permanent magnet-assisted synchronous reluctance generator (PMa-SynRG) can be a good solution for low cost, high efficiency and reliable generator systems due to its increased reluctance torque component [2-3]. A PMa-SynRG has the potential of being a high efficiency drive by utilizing the proper amount of magnet and reluctance torque. This work suggests a PMa-SynRG with two flux barriers and permanent magnets embedded in the second layer of the rotor. NdFeB was used as permanent magnets in the rotor to prevent demagnetization [4-7]. The rotor structure and the concentrated winding configuration of a 3kW PMa-SynRG is shown in Fig. 1.

The drive system consists of a back-to-back pulse width modulation (PWM) voltage-fed drive. Fig. 2 depicts a back-to-back converter where a three-phase PWM rectifier is used at the alternator output to generate a fixed DC bus voltage. A single-phase PWM inverter is used to interface with the utility grid. In this case, because of the front-end PWM rectifier it is possible to control the alternator currents such that maximum power is delivered by the generator at any speed. Therefore, the fuel consumption can be minimized by operating the internal combustion engine at its sweet spot for any load [8-9].

† Corresponding Author: School of Electrical and Electronics Engineering, Chungang University, Seoul, Korea. (sskwak@cau.ac.kr)
* School of Electrical, Electronics and Communication Engineering, Korea University of Technology & Education, Cheonan, Korea. (jhbaek@koreatech.ac.kr)
Received: July 17, 2017; Accepted: November 9, 2017

Generator power can be controlled by the maximum power per voltage function block while the input power command is decided by means of measuring the DC link voltage. These features make the current and voltage-fed drive using direct power control a good candidate for driving any type of synchronous generators including the proposed PMa-SynRG [10-12]. In this paper, the virtual flux based direct power control (VF-DPC) strategy with space vector

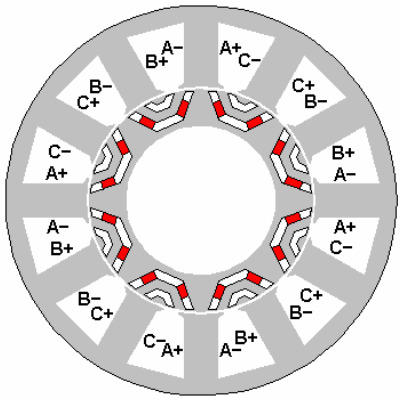

Fig. 1. Cross section of a PMa-SynRG with concentrated winding

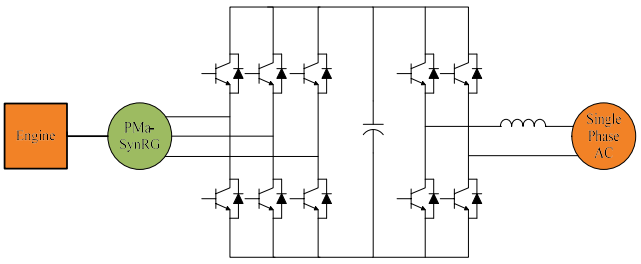

Fig. 2. Back-to-back PWM voltage-fed drive

modulator (SVM) is used for the PMa-SynRG system because it can control the output power directly and it has lower sampling frequency than that of current vector control [13-14]. The VFDPC has disadvantages such as variable switching frequency and high sampling frequency required of hysteresis comparator. In the constant speed operation such as auxiliary generator system, these drawbacks can overcome by simple algorithm using SVM for unity power control.

2. Proposed Control Method

The direct power control techniques for PWM rectifiers can generally be classified as voltage-based and virtual flux-based methods. In voltage-based direct power control, the real and reactive powers drawn from the power line are calculated using information about the dc-link voltage, rectifier state and line currents. The unity power factor condition requires that the reactive power to be zero. The DC link voltage based on direct power control principle resembles the field oriented control. The use of hysteresis controller for direct selection of the converter switching states in the direct power control is simple for the direct power control method. The virtual flux vector is defined as the time integral of the phase voltage vector. It has been proposed to improve the rectifier control under non-ideal supply voltage conditions [15], taking advantage of the integrator's low-pass filter properties. In the virtual flux-based direct power control, the line voltage is estimated as the sum of rectifier input voltage and voltage drop across the line reactors.

In this paper, the virtual flux-based approach is proposed to improve the dc link voltage oriented control. In stationary $\alpha-\beta$ coordinates, the integration of the line-to-line voltage leads to line flux vector. Fig. 3 shows the block diagram of the proposed virtual flux-based direct power control system where the commands of reactive power Q_{ref} set to zero for unity power factor and active power P_{ref} are compared with the estimated active, reactive powers. The digitized output signals of the hysteresis controller d_p and d_q decide the switching states of the voltage vector. The converter voltage and the virtual flux are calculated from measuring the dc link voltage and the switches states in the virtual flux estimator block. The estimated line currents and the virtual flux parameters are delivered to the active and reactive power estimator block. The virtual flux-based power estimation has advantages of low sampling frequency(10kHz), simple algorithm and low THD [16].

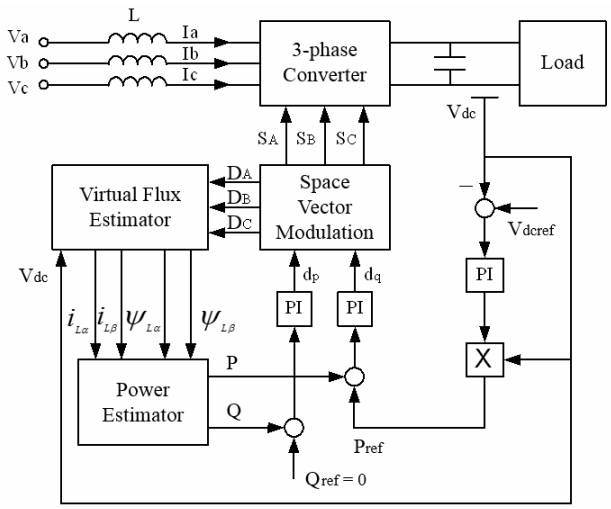

Fig. 3. Block diagram of power estimation based on virtual flux

The power estimation based on the DC link voltage is very simple but it has several disadvantages such as need for high sampling frequency and high error of the estimated value. The virtual flux based approach has been proposed to improve the DC link voltage oriented control method [18, 19]. In the stationary $\alpha-\beta$ coordinates, the integration of the line-to-line voltage leads to a line flux vector given by,

$$\Psi_L = \int V_L dt \tag{1}$$

where

$$\begin{bmatrix} V_{L\alpha} \\ V_{L\beta} \end{bmatrix} = \sqrt{\frac{2}{3}} \cdot \begin{bmatrix} 1 & \frac{1}{2} \\ 0 & \frac{\sqrt{3}}{2} \end{bmatrix} \begin{bmatrix} V_{ab} \\ V_{bc} \end{bmatrix} \tag{2}$$

$$\begin{bmatrix} I_{L\alpha} \\ I_{L\beta} \end{bmatrix} = \sqrt{\frac{2}{3}} \cdot \begin{bmatrix} \frac{3}{2} & 0 \\ \frac{\sqrt{3}}{2} & \sqrt{3} \end{bmatrix} \begin{bmatrix} I_a \\ I_b \end{bmatrix} \tag{3}$$

The virtual fluxes components are calculated by the DC link voltage V_{dc} and the duty cycle of modulator D_a, D_b, D_c in the virtual flux estimator block are given by,

$$\Psi_{L\alpha} = \int \left[\sqrt{\frac{2}{3}} V_{dc} \left(D_a - \frac{1}{2}\left(D_b + D_c\right) \right) \right] dt + LI_{L\alpha} \tag{4}$$

$$\Psi_{L\beta} = \int \left[\frac{1}{\sqrt{2}} V_{dc} \left(D_b - D_c \right) \right] dt + LI_{L\beta} \tag{5}$$

For balanced line voltages, the instantaneous active and reactive powers can be calculated as using complex notation, the instantaneous power can be calculated by,

$$\mathrm{V}_L \cdot I_L^* = \left[\frac{d}{dt} \Psi_L \mid_\alpha + j \frac{d}{dt} \Psi_L \mid_\beta + j\omega \left(\Psi_{L\alpha} + j\Psi_{L\beta} \right) \right] \tag{6}$$

where * denotes conjugate of the line current.

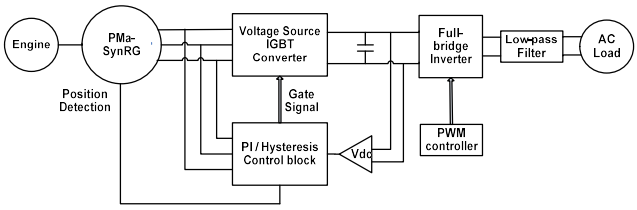

Fig. 4. Block diagram of power estimation based on the DC link voltage

By derivatives of the sinusoidal balanced virtual flux are zero, the instantaneous active and reactive power can be calculated.

$$P = \omega \cdot (\Psi_{L\alpha} I_{L\alpha} - \Psi_{L\beta} I_{L\beta}) \quad (7)$$

$$Q = \omega \cdot (\Psi_{L\alpha} I_{L\alpha} + \Psi_{L\beta} I_{L\beta}) \quad (8)$$

Fig. 4 shows the block diagram of voltage source IGBT converter with full bridge PWM inverter for generating the single-phase AC output. The measured three-phase PMa-SynRG back-EMF and current are input of the control block for generating the optimal current reference for obtaining maximum output power. The PWM rectifier basically operates as a boost chopper at the input. The control principle of the PWM rectifier for sinusoidal line current at unity power factor is shown in the block diagram. The command DC link voltage is compared with the actual DC link voltage and the error signal through a PI controller is multiplied with the line voltage waveform to generate the line current command.

3. Simulation Results

In order to verify the operation of the virtual flux based direct power control, the PWM rectifier with the PWM inverter control scheme has been simulated using PSIM. The line current and $\alpha-\beta$ coordinate current waveforms are shown in Fig. 5. The $\alpha-\beta$ coordinate currents are calculated from phase A and B.

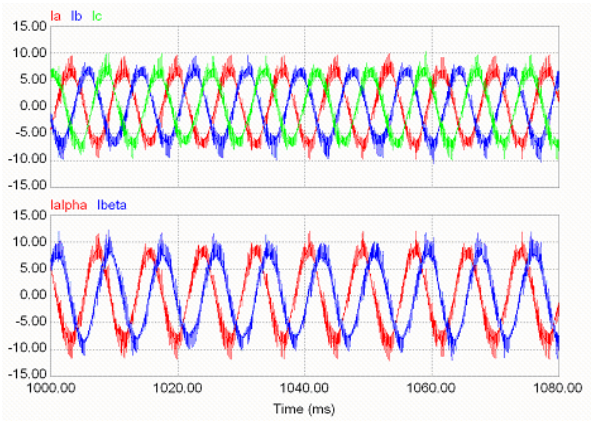

Fig. 5. Line current and $\alpha-\beta$ coordinate current waveforms

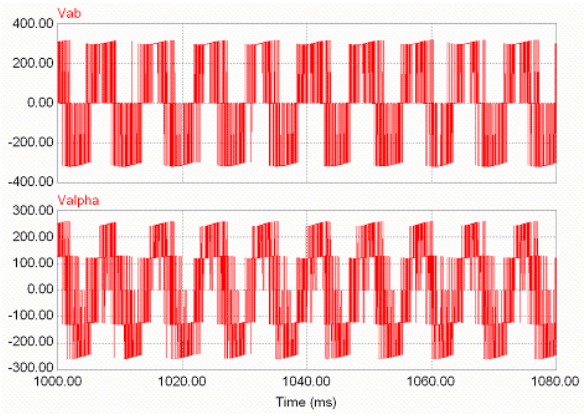

Fig. 6. Line-to-line voltage and alpha coordinate voltage

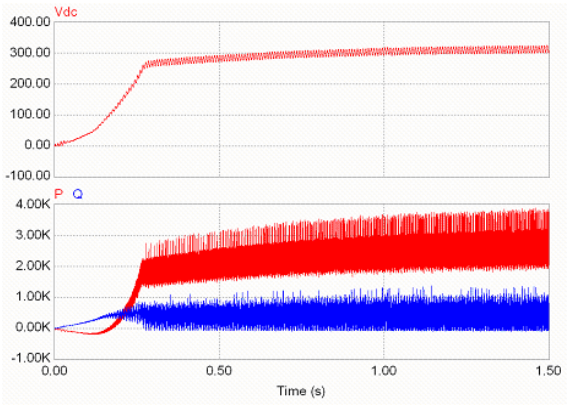

Fig. 7. DC link voltage, output active and reactive powers

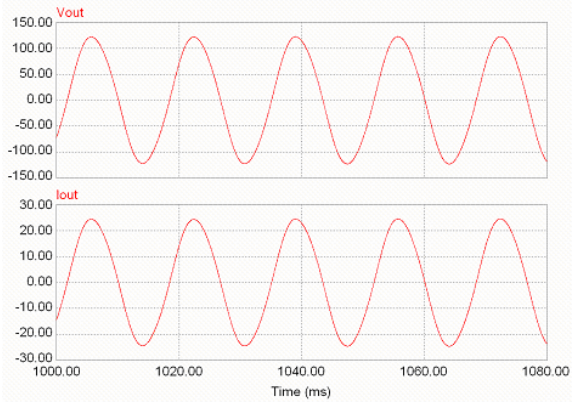

Fig. 8. AC output current and voltage waveforms.

The line-to-line voltage and alpha coordinate voltage are shown in Fig. 6. The integration of the line-to-line voltage leads to a line flux vector and the converter voltage and virtual flux are calculated from the DC link voltage and the switch states in the virtual flux estimator block. Using the DC link voltage command, the active power command is generated by the PI controller and the commanded 3kW active power is achieved at a DC bus voltage equal to 300Vdc. It is shown in Fig. 7.

Using a single-phase PWM inverter and the accom-

panying low pass filter, this system can deliver the required sinusoidal 60Hz, 120V single-phase output. The single-phase output voltage and current are shown in Fig. 8 and this voltage-fed VF-DPC system can supply 3kW output power, at 120V with 25A single phase current.

4. Experimental Results

4.1 Experimental setup

Fig. 9 shows the 3kW PMa-SynRG test bed. A 7.5hp three phase induction motor controlled by an Allen-Bradley 1336 plus adjustable frequency AC drive runs at 3,600 rpm constant speed and works as the prime mover. The fabricated 3kW PMa-SynRG is directly coupled to the induction motor.

The supply frequency of the induction motor is 60Hz and therefore it runs close to 3,600rpm and the PMa-SynRG generated frequency is around 240Hz because the induction motor has two poles and the PMa-SynRG has eight poles. In order to detect the mechanical rotating position, an encoder installed on the PMa-SynRG shaft is being used. The fabricated test bed for the 3kW PMa-SynRG is shown in Fig. 10. The adjustable frequency AC drive is programmed to keep the constant speed (3,600rpm) of the three-phase induction motor. The 3kW PMa-SynRG is working as a generator; the phase conductors are connected to the three phase rectifier and voltage sensors.

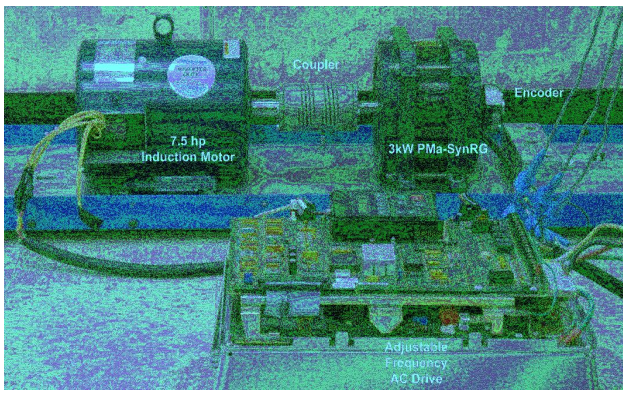

Fig. 9. Fabricated 3kW PMa-SynRG test bed

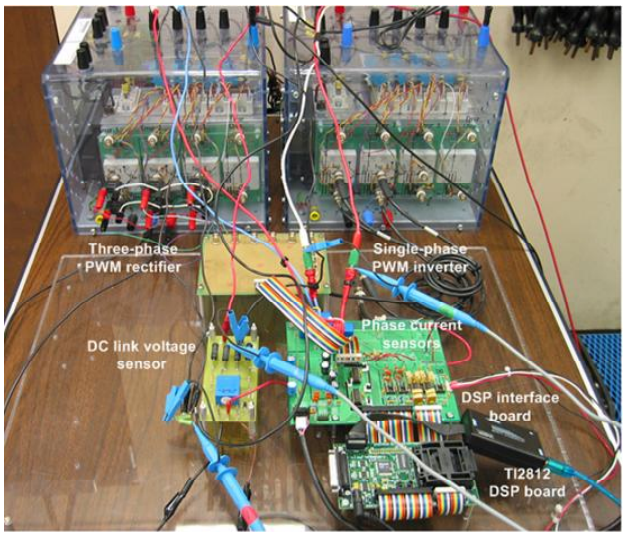

Fig. 10. Experimental setup for the back-to-back PWM control system

Fig. 10 shows the experimental setup for the back-to-back PWM drive system. For the back-to-back PWM drive, two IGBT modules are being used for the three-phase PWM rectifier and the single phase PWM inverter.

In order to implement the direct power control algorithm with the voltage-fed PWM drive, one voltage sensor and two current sensors are used and TI2812 DSP is used as the main contoller. For detecting the mechanical rotating position, an encoder is being used and it is installed on the PMa-SynRG shaft. The overall experimental setup is shown in Fig. 11. The three-phase AC source is connected to the adjustable frequency AC drive in order to control the three-phase induction motor. A DC power source is used for both the interface board and the voltage-fed PWM converters. The 3kW generator setup is controlled by the direct power control system using the DSP board. In order to supply 60Hz/120V single phase output, the generator test bed connected to the three-phase rectifier and the rectified DC link voltage supplies the single phase output voltage to the resistor panel.

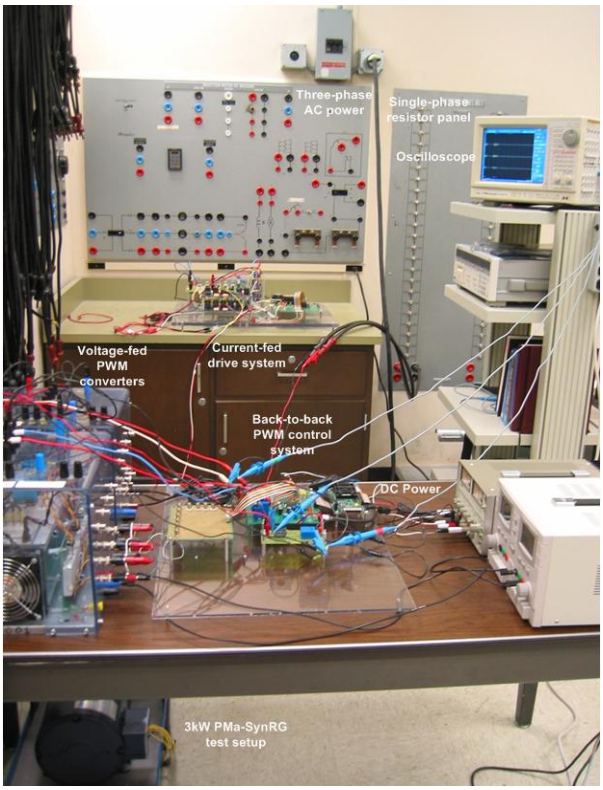

Fig. 11. Overall experimental setup for the voltage-fed PWM drive system

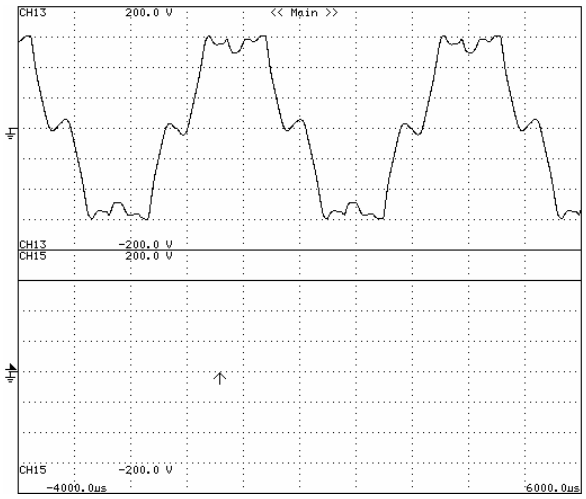

Fig. 12. Experimental waveforms of input voltage and DC link voltage with no load (Top to bottom: (a) line-to-line voltage Vab (50V/div) (b) DC link voltage (50V/div))

Fig. 13. Experimental waveforms of DC link voltage and phase current with no load (Top to bottom: (a) DC link voltage (50V/div) (b) phase current (10A/div))

4.2 Experimental waveforms

4.2.1 Three-phase PWM Rectifier at No-load and Diode Rectification

When PWM gate signals for transistors are not fired, free-wheeling diodes in IGBTs are conducted and this circuit work as a three-phase diode rectifier. In this case, the DC link voltage is the same as the peak value of the line-to-line input voltage. The big DC link capacitor purifies the three-phase input voltage to the ripple free DC link voltage. In the experiment, the three-phase voltage-fed PWM rectifier under load and no-load conditions using diode rectifier are verified. The peak value of the line-to-line voltage is 150V and the line-to-neutral voltage is 87V.

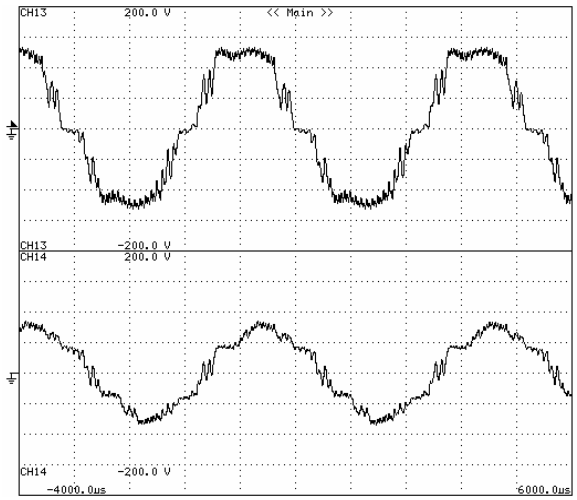

Fig. 14. Experimental waveforms of input voltages with DPC (Top to bottom: (a) line-to-line voltage Vab (50V/div), (b) line-to-neutral voltage Va (50V/div))

Therefore, the DC link voltage is 150V using the three-phase diode rectifier under no-load condition.

When the resistive load is connected to the DC link, phase currents are flowing through diodes and the output voltage is decreased from 150V to 130V. The 20V voltage drop is across the generator phases and connecting resistances. The peak value of the phase current is 30A and the DC link current is around 25A. Therefore, the DC link power from the generator is 3,250W. This result is close to the maximum output power of the PMa-SynRG. Fig. 14 shows the experimental waveforms of the DC link voltage and the phase current under load.

4.2.2 Three-phase PWM Rectifier with Direct Power Controller

For the direct power controller, two current sensors and one DC link voltage sensor are being used to calculate the virtual flux. In the experiment, the virtual flux is calculated by the integrator in the DSP program. To prevent the saturation in the DSP program, the hi-pass filter is applied after the integrator. The estimated line currents and virtual flux parameters are delivered to the active, reactive power estimator block. The estimated active and reactive powers are compared with the command for the hysteresis controller and the output signal of the hysteresis controller decide the switching table for the voltage vector.

Figs. 14 and 15 show the experimental results when the active power command is 3kW and the reactive power command is zero. From the DPC controller, the DC link output voltage is 145V and the current is 21A. Therefore, the calculated DC link output power is 3,045W. (50V/div)

In order to verify the direct power control algorithm, another power operating point such as 2kW output power is selected. When the power command decreases to 2kW and the reactive power command is zero, the DC link

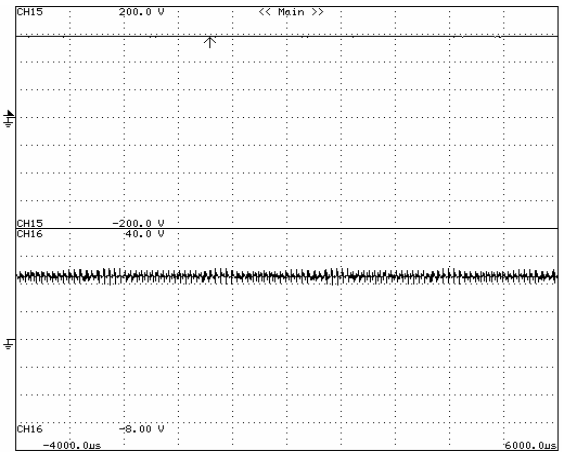

Fig. 15. Experimental waveforms of input voltages with DPC (Top to bottom: (a) DC link output voltage (50V/div) (b) DC link output current (10A/div))

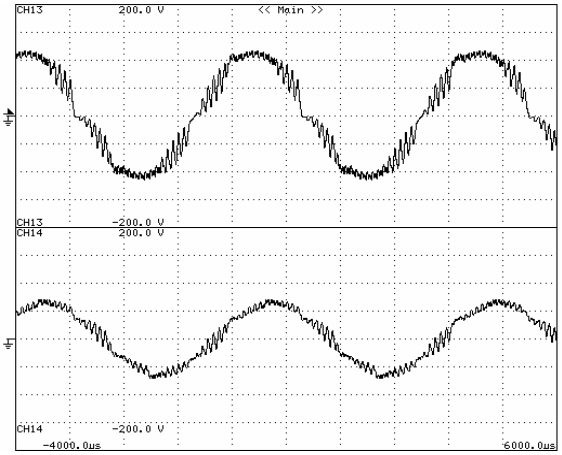

Fig. 16. Experimental waveforms of input voltages with DPC (Top to bottom: (a) line-to-line voltage Vab (50V/div), (b) line-to-neutral voltage Va (50V/div))

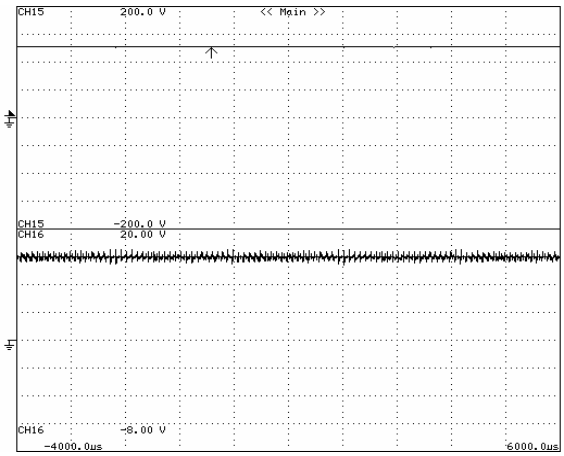

Fig. 17. Experimental waveforms of DC link output voltage and current with DPC (Top to bottom: (a) DC link output voltage (50V/div) (b) DC link output current (5A/div))

Table 1. Experimental results

	DC link voltage	DC link current	DC link power
No DPC	130V	25A	3,250W
30kW DPC	145V	21A	3,045W
20kW DPC	130V	15A	1950W

output voltage is decreased to 130V and current is decreased to 15A. From this result, the DC link output power is 1,950W. The controlled output results are shown in Figs. 16 and 17.

5. Conclusions

This research has investigated the direct power control algorithm for 3kW generator system. The proposed converter topology and control algorithm improve generator performance for the designed 3kW PMa-SynRG system.

A virtual flux-based direct power control is proposed in order to control the output power directly in the voltage-fed drive. The goal of the direct power control is to maintain the required output power operating point. The direct power control has advantages such as a simple algorithm at fixed operating speed and a good dynamic response for the voltage-fed drive. Simulation and experimental results verify the developed control algorithm and shows good performance for the 3kW PMa-SynRG system.

Acknowledgements

This work was supported by Educational Research Promotion Funding in Koreatech and the Human Resources Development (No.20174030201810) of the Korea Institute of Energy Technology Evaluation and Planning(KETEP) grant funded by the Korea government Ministry of Trade, Industry and Energy.

References

[1] J. Wai, and T.M. Jahns, "A new control technique for achieving wide constant power speed operation with an interior PM alternator machine," in *Conf. Rec. IEEE IAS Annu. Meeting*, vol. 2, pp. 807-814, Oct. 2001.

[2] H. Murakami, Y. Honda, and H. Kiriyama, "The performance comparison of SPMSM, IPMSM and SynRM in use as air-conditioning compressor," in *Conf. Rec. IEEE IAS Annu. Meeting*, vol. 2, pp. 840-845, Oct. 1999.

[3] H. Murakami, Y. Honda, H. Kiriyama, S. Morimoto, and Y. Takeda, "The performance comparison of SPMSM, IPMSM and SynRM in use as air-

conditioning compressor," in *Conf. Rec. IEEE IAS Annu. Meeting*, vol. 2, pp. 840-845, Oct. 1999.
[4] S. Morimoto, M. Sanada, and Y. Takeda, "Performance of PM assisted synchronous reluctance motor for high efficiency and wide constant power operation," *IEEE Trans. Ind. Appl*., vol. 37, no. 5, pp. 1234-1240, Sept./Oct. 2001.
[5] P. Niazi, H.A. Toliyat, D-H. Cheong, and J-C. Kim, "A low-cost and efficient permanent magnet assisted synchronous reluctance motor drive," *IEEE Trans. Ind. Appl*., vol. 43, no. 2, pp. 542-550, Mar./Apr. 2007.
[6] I. Boldea, L. Tutelea, and C. I. Pitic, "PM assisted reluctance synchronous motor/generator (PM-RSM) for mild hybrid vehicle: electromagnetic design," *IEEE Trans. Ind. App*., vol. 40, no. 2, pp. 492-498, Mar./Apr. 2004.
[7] T. Nakamura, S. Morimoto, M. Sanada, and Y. Takeda, "Optimum control of IPMSG for wind generation system," *Proc. PCC*, vol. 3, pp. 1435-1440, Apr. 2002.
[8] R. Q. Machado, J. A. Pomilio, and E. G. Marra "Electronically controlled bi-directional connection of induction generator with a single-phase grid," *Ind. Elec. Soc. IECON*, vol. 3, pp. 1982-1987, Nov./Dec. 2001.
[9] M. Chinchilla, S. Arnaltes, and J.C. Burgos, "Control of permanent-magnet generators applied to variable-speed wind-energy systems connected to the grid," *IEEE Trans. En. Conv*., vol. 21, no. 1, pp. 130-135, Mar. 2006.
[10] J.H. Lee, J.C. Kim, and D.S. Hyun, "Effect analysis of magnet on Ld and Lq inductance of permanent magnet assisted synchronous reluctance motor using finite element method," *IEEE Trans. Magnetics*, vol. 35, no. 35, pp. 1199-1206, May 1999.
[11] B.J. Chalmers, S.A. Hamed, and G. D. Baines, "Parameters and performance of a high-field performance permanent-magnet synchronous motor for variable-frequency operation," *Proc. IEE*, vol. 132, pt. B, pp. 117-124, 1985.
[12] J. Baek, M.M. Rahimian, and H.A. Toliyat, "Optimal design and comparison of stator winding configurations in permanent magnet assisted synchronous reluctance generator," *in Conf. Rec. IEEE IEMDC*, pp. 732-737, May 2009.
[13] D. Seyoum, and C. Grantham, "Terminal voltage control of a wind turbine driven isolated induction generator using stator oriented field control," *in Conf. Rec. IEEE APEC*, vol. 2, pp. 846-852, Feb. 2003.
[14] M. Malinowski, W. Kolomyjski, M.P. Kazmierkowski, and S. Stynski "Control of variable-speed type wind turbines using direct power control space vector modulated 3-level PWM converter," *in Conf. Rec. Ind. Tech. ICIT*, pp. 1516-1521, Dec. 2006.
[15] J. Zhang, F. Rahman, and C. Grantham "A new scheme to direct torque control of interior permanent magnet synchronous machine drives for constant inverter switching and low torque ripple," in *Conf. Rec. PEMC*, vol. 3, pp. 1-5, Aug. 2006.
[16] M. Malinowski, M. Jasinski, and M.P. Kazmierkowski, "Simple direct power control of three-phase PWM rectifier using space-vector modulation (DPC-SVM)," *IEEE Trans. Ind. Elec*., vol. 51, no. 2, pp. 447-454, Apr. 1991.
[17] J. Zhang, M.F. Rahman, and C. Grantham, "A new scheme to direct torque control of interior permanent magnet synchronous machine drives for constant inverter switching frequency and low torque ripple," in *Conf. Rec. CES/IEEE IPEMC*, vol. 3, pp. 1-5, Aug. 2006.
[18] M. Malinowski, M.P. Kazmierkowski, and A.M. Trzynadlowski, "A comparative study of control techniques for PWM rectifiers in AC adjustable speed drives," *IEEE Trans. Power Elec*., vol. 18, no. 6, pp. 1390-1396, Nov. 2003.
[19] P. Niazi, H.A. Toliyat, and A. Goodarzi, "Robust maximum torque per amp (MTPA) control of PM assisted SynRM for tractions application," *IEEE Trans Power Elec*., vol. 56, no. 4, pp. 1538-1545, July 2007.
[20] S. Morimoto, Y. Takeda, T. Hirasa, and K. Taniguchi, "Expansion of operating limit for permanent magnet motor by current vector control considering inverter capacity," *IEEE Trans. Ind. Appl*., vol. 26, no. 5, pp. 866-871, Sep./Oct. 1990.
[21] S. Morimoto, H. Kato, M. Sanada, and Y. Takeda "Output maximization control for wind generation system with interior permanent magnet synchronous generator," in *Conf. Rec. IEEE IAS Annu. Meeting*, vol. 1, pp. 503-510, Oct. 2006.

Jeihoon Baek received M.S. degrees in electrical engineering from University of Wisconsin-Madison, Madison, WI, USA, in 2006, and the Ph.D. degree in electrical engineering from Texas A&M University, College Station, TX, USA, in 2009. From 1998 to 2000, he was with Amotech, Seoul. He was also with Samsung Electro-mechanics, Suwon, Korea, as a Senior Research Engineer from 2000 to 2003. From 2010 to 2013, he worked as a Principal Engineer at Samsung Advanced Institute of Technology, Youngin, Korea. He was also with Korea Railroad Research Institute, Uiwang, Korea, as a Senior Research Engineer from 2014 to 2016. Since 2017, he has been with Korea University of Technology and Education, Cheonan, Korea, currently as an Assistant Professor. His current research interests and experiences include the design and analysis of electrical

machines, variable speed drives for traction and propulsion applications, and novel power conversion topology.

Sangshin Kwak received the Ph.D. degree in Electrical Engineering from Texas A&M University, College Station, Texas in 2005. From 1999 to 2000, he worked as a research engineer at LG Electronics, Changwon, Korea. He was also with Whirlpool R&D Center, Benton Harbor, MI, in 2004. From 2005 to 2007, he worked as a Senior Engineer in Samsung SDI R&D Center, Yongin, Korea. From 2007 to 2010, he worked as an assistant professor at Daegu University, Gyeongsan, Korea. Since 2010, he has been with Chung-ang University, Seoul, Korea, currently as a professor. His research interests are topology design, modeling, modulation, and control of power converters, multilevel converters, renewable energy systems, and power quality.